SPE-185795-MS

Step Rate Test as a Way to Understand Well Performance in Fractured Carbonates

A. Shchipanov and L. Kollbotn, IRIS; M. Prosvirnov, ConocoPhillips

Copyright 2017, SPE Europec featured at 79th EAGE Conference and Exhibition

This paper was prepared for presentation at the SPE Europec featured at 79th EAGE Conference and Exhibition held in Paris, France, 12–15 June 2017.

This paper was selected for presentation by an SPE program committee following review of information contained in an abstract submitted by the author(s). Contents of the paper have not been reviewed by the Society of Petroleum Engineers and are subject to correction by the author(s). The material does not necessarily reflect any position of the Society of Petroleum Engineers, its officers, or members. Electronic reproduction, distribution, or storage of any part of this paper without the written consent of the Society of Petroleum Engineers is prohibited. Permission to reproduce in print is restricted to an abstract of not more than 300 words; illustrations may not be copied. The abstract must contain conspicuous acknowledgment of SPE copyright.

Abstract

Step Rate Test (SRT) is commonly used to estimate formation parting (or fracture opening) pressure for stimulated wells. SRTs may also focus on changes of well performance at different rates / pressures that is of special interest for stress-sensitive reservoirs such as fractured carbonates. Installation of permanent downhole gauges (PDG) and running SRTs on injection wells at the Ekofisk field gave a chance to improve the understanding of reservoir and well performance. Analysis of these SRTs also resulted in further development of SRT interpretation techniques.

An approach to SRT interpretation, combining analytical pressure-rate (p-Q) curve analysis and step-by-step Pressure Transient Analysis (PTA) with numerical simulation of SRT, was suggested and tested. Applying this approach to Ekofisk SRTs has shown that the p-Q analysis may be used for diagnostics of well performance changes, while step-by-step PTA enables decomposing of well (skin factor) and reservoir (conductivity) effects with estimation of corresponding well-reservoir parameters as pressure or rate functions. Numerical simulation confirmed that pressure dependent conductivity estimated from the step-by-step PTA is the governing factor in matching SRT history.

Special attention was paid to the uniqueness of SRT interpretation using suggested approach. Reaching infinite acting radial flow (IARF) regime at each step of a test provided unique parameter estimates as shown by example of a stimulated slanted injector. Being too far from IARF at end of each step will make the interpretations more uncertain. Different sets of changing parameters estimated from SRT interpretation could provide satisfactory match in numerical runs as was illustrated by example of a horizontal injector with multiple induced fractures. Comparison of interpretation results for different wells integrating additional field data is a possible way to reduce this uncertainty.

Finally, some hints to designing, conducting and interpreting SRTs of different types of wells in fractured carbonate fields are given, using Ekofisk field experience.

Introduction

Step-rate tests (SRTs) are traditionally used for evaluating fracturing (reservoir parting) pressure and efficiency of well treatments, when an induced fracture is generated by high pressure injection (Singh, Agarwal, & Krase, 1987), (Salazar & Kumar, 1992), (Lacy & Hudson, 1995). The simplest way of

Downloaded from http://onepetro.org/SPEEURO/proceedings-pdf/17EURO/2-17EURO/D021S001R004/1290734/spe-185795-ms.pdf/1 by Sharisse Geiger on 01 March 2024

estimating the fracturing pressure is analysis of well bottom hole pressure (maximum value for a step) versus flow rate resulted from an SRT, also known as *p-Q* plot. Appearance of two linear intersecting trends in the plot gives reliable estimate for the fracturing (for generated induced fracture) or fracture opening (for pre-existing fracture) pressure. SRTs are often followed by a reduced rate step or well shut-in with pressure fall-off, which may be interpreted to estimate fracture closure pressure (also known as 'mini-frac' test and after-closure analyses (Craig & Blasingame, 2006)). An SRT may consist of monotonically increasing (step-up) or decreasing (step-down) rate steps or their combination depending on objectives of the test and parameters of interest, being parting, fracture opening or closure pressures, rate dependent skin, instant shut-in pressure, leak-off coefficient *etc.* (Elshahawi & Gad, 2001), (Lizak, Bartko, Self, Izquierd, & Al-Mumen, 2006).

In general, SRTs may be used for evaluating any changes in well and reservoir parameters with changing pressure and rate. Pressure Transient Analysis (PTA) may be used to interpret well-reservoir parameters at each step of an SRT, while comparison of pressure responses at different steps may help in revealing changes in these parameters (Singh & Agarwal, 1990).

For stress-sensitive formations, SRTs may be applied to disclose changes in permeability due to pressure changes. Using SRTs for this purpose was reported in the literature, in particular for the Ekofisk based study (Economides, Buchsteiner, & Warpinski, 1994).

Using horizontal wells has become general practice for improving sweep efficiency and oil recovery. These are of special interest for low permeability formations, where additional stimulation is often required. Interpretation of well test data for such wells can be difficult and uncertain (Houze, Viturat, & Fjaere, 2011). The complications are generally related to different well segments penetrating reservoirs with varying properties (porosity / permeability), as well as multiple induced fractures having different properties and performance. Multi-fracture horizontal well simulations have shown that response from multiple fractures is often similar to a single fracture response as superposing of linear flows takes place (Hegre & Larsen, 1994), (Egya, et al., 2016). Interpretation of pressure measurements from a gauge usually installed above perforations deals with an average well-reservoir response, and separating effects from different reservoir zones and fractures is a challenge. The uncertainty in interpretation of horizontal well responses is also related to stimulation effects, and wells being longer than the inter-well spacing, where the first may mask early radial flow to the well, while the second - preventing late radial flow. In such cases, observing reliable radial flow regimes with stabilized pressure derivatives is the key point in achieving unique interpretations.

In this paper, an approach for interpretation of SRTs, combining detection of well injectivity (productivity) changes from simple *p-Q* analysis with analyses of pressure transients from each rate step to separate changes in well and reservoir parameters is described and tested on Ekofisk field data. The application of step-by-step PTA is similar to the time-lapse PTA earlier discussed by the authors (Shchipanov, Berenblyum, & Kollbotn, 2014). Two examples of SRT interpretations for slanted and horizontal wells, followed by numerical simulation of the SRTs on segment models, are used to show capabilities and limitations of both *p-Q* analysis and step-by-step PTA. Special attention is paid to uncertainties with SRT interpretations for horizontal stimulated wells and to integration of the analytical interpretation results into reservoir simulation making history matching of SRTs easier and more reliable.

Step Rate Test (SRT): A general overview for vertical and horizontal stimulated wells in pressure-sensitive reservoirs

p-Q plot for the cases of constant, growing and declining well performance

The simplest way of introducing productivity or injectivity index (*PI* or *II*) of a well is to determine it as a ratio of well flow rate and difference between current flowing pressure and initial (or average) pressure in the reservoir segment containing the well (relationships *(1)-(3)* in the appendix). Based on this determination, constant *PI* provides a straight line in pressure versus rate or *p-Q* plot (Figure 1). Growing *PI* causes

Downloaded from http://onepetro.org/SPEEURO/proceedings-pdf/17EURO/2-17EURO/D021S001R004/1290734/spe-185795-ms.pdf/1 by Sharisse Geiger on 01 March 2024

convexity of *p-Q* plot to the pressure axis, while declining *PI* - convexity to the rate axis (Figure 1). This simple *PI* concept is often used by reservoir engineers in everyday practice providing a reasonable basis for monitoring well performance and comparison of different wells.

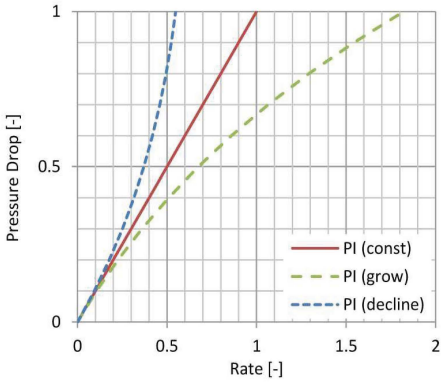


Figure 1—Pressure drop versus rate (p-Q) plot as determined by equation (1) in the appendix for constant, increasing and decreasing Productivity Indices (PI).

Step Rate Tests (SRTs), consisting of sequential steps of increasing rate (Figure 2) are usually utilized to construct *p-Q* plots. While interpreting such plots, it is normally assumed that if well-reservoir parameters such as skin and permeability-thickness product (*kh*) remain the same at each step, a linear or close to linear *p-Q* plot should be expected. In practice, however, noisy data may often cause deviations from a linear *p-Q* trend even without any variation in well-reservoir parameters at different steps. Also, the initial (or average) reservoir pressure used in the *PI* estimations is not necessarily constant, while superposing steps on top of each other may lead to significant deviation from linear *p-Q* plot as discussed in the next section.

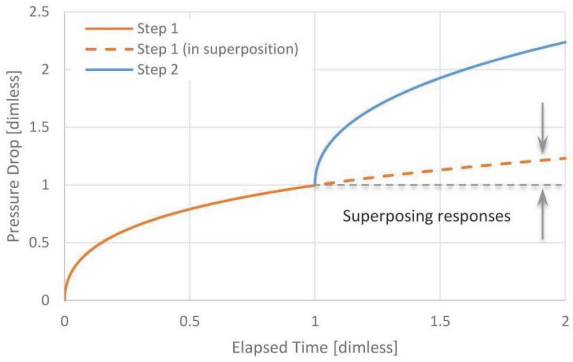


Figure 2—Two sequential steps of Step-Rate Test (SRT): superposing response of first step on second step causes additional pressure drop at the second step.

Superposing steps and impact on *p-Q* plot

An SRT may be considered as overlaying an additional rate on top of previous one, known in PTA as rate superposition (Bourdet, 2002). Mathematically, the superposition principle makes it possible to simulate pressure response to a variable rate history. Considering two sequential rate steps (Figure 2), the pressure response on the second step may be divided into two components: (1) continuation of the response from the first step and (2) response to the rate increase at the second step. The relative significance of the first and second components for the current step is mainly governed by the flow regime occurring at the end of the previous step. If a steady-state flow regime (e.g. with constant pressure boundary) is reached at the previous

Downloaded from http://onepetro.org/SPEEURO/proceedings-pdf/17EURO/2-17EURO/D021S001R004/1290734/spe-185795-ms.pdf/1 by Sharisse Geiger on 01 March 2024

step, the first component is negligible. If the previous step is still in the Infinite Acting Radial Flow (IARF) regime, the first component will be noticeable, but usually significantly smaller than the second one. On the other hand, transitional (*e.g.* linear) flow regimes can make the first component comparable to the second one. In *p-Q* plots, the first component governs the deviation from a straight line (Figure 3). As illustrated by *p-Q* plots resulted from analytical simulations, reaching IARF at each step of the SRTs for both vertical and horizontal wells as long as they are not stimulated provided *p-Q* response that is close to the dashed straight line. When well is stimulated (described via negative skin), the transitional flow occurs at each step (IARF is not reached) causing significant deviation from the *p-Q* straight line. This should be taking into account when interpreting SRTs of stimulated wells, especially the horizontal ones.

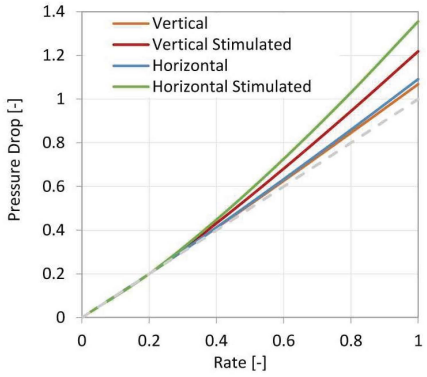


Figure 3—Normalized p-Q plot for synthetic vertical and horizontal wells and the same wells with stimulation (induced fracture): deviation from the straight line due to superposing responses of sequential steps (Figure 2).

Well stimulation via induced fracturing and skin concept

As mentioned, the flow regimes during rate steps have significant influence on SRT interpretation, in particular on analysis of the *p-Q* plot. Since many production and injection wells today are stimulated (including those analyzed hereafter), the impact of well stimulation on simulated pressure response is particularly interesting.

Figure 4 shows synthetic pressure responses obtained with analytical models, using three alternative approaches to model well stimulation resulted in a negative skin. All cases gave the same final skin (-5), as illustrated by the similarity of derivative and pressure drop when the IARF regime is reached (after 10 *hr*). Yet, the pressure and derivative behavior could be quite different before the IARF regime is reached, depending on how the well stimulation effects are interpreted and modeled.

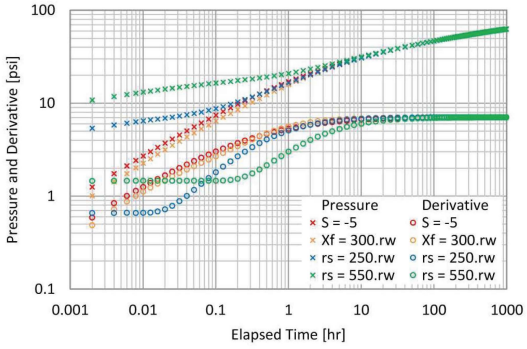


Figure 4—Pressure and derivative transients for vertical well with skin: S = -5, and two other models providing the same total skin: infinite conductivity fracture (Xf = 300·rw) and composite reservoir with radii of the enhanced permeability zone of 250·rw and 550·rw.

Downloaded from http://onepetro.org/SPEEURO/proceedings-pdf/17EURO/2-17EURO/D021S001R004/1290734/spe-185795-ms.pdf/1 by Sharisse Geiger on 01 March 2024

The model with skin and that with induced fracture gave similar responses, exhibiting a period of increasing derivatives before it becomes constant (indicating an IARF regime, Figure 4). This happened although the flow regimes are quite different for these two cases. The skin is usually included in the pressure diffusivity equation by modifying well radius to be equal to the effective radius calculated from the skin (Bourdet, 2002). In this case, the length of the increasing derivative period is proportional to the effective well radius. In the case of induced fracture, increasing derivative reflects linear flow to the fracture. In an alternative model of composite reservoir (Figure 4), the same total negative skin was provided applying two sets of the model parameters describing enhanced flow capacity in the near wellbore area: a smaller area with larger capacity and vice versa. These provided dissimilar derivatives (depending on the inner area' radius and flow capacity), which again were different from the two cases described above. Also, as shown in Figure 5, the same total skin (pressure drop) may be obtained for the late response (after 10 *hr*) via increasing fracture half-length in combination with additional growing fracture skin. In this case, the derivatives during the early response would depend on the fracture half-length. These examples illustrate the fact that an actual pressure response and derivative may be matched with different models of stimulated well.

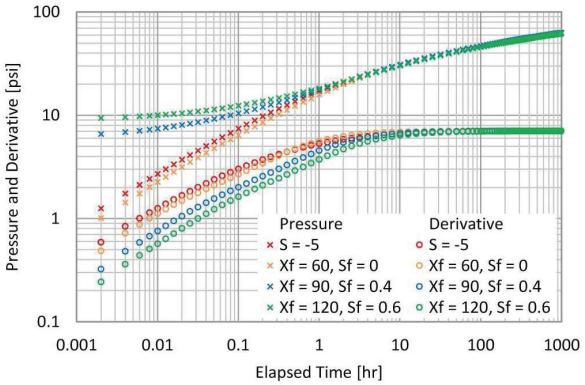


Figure 5—Simulated responses from Figure 4 (S = -5 and Xf = 300·rw = 60 ft) compared with two responses of longer fractures (Xf = 90 and 120 ft) but with increasing fracture skin (0.4 and 0.6). All models provide total skin of -5.

A note on non-linear pressure diffusivity and SRTs in pressure sensitive reservoirs

Reservoir response in the case of pressure (actually stress) sensitive permeability is quite different from that of constant permeability. The sensitivity of permeability to pressure creates non-linearity (self-dependency) in the pressure diffusivity equation describing reservoir fluid flow, even in the single-phase flow case. These non-linearity effects are illustrated in Figure 6. In the case of constant permeability, the equal stepping in rate generates close to equal stepping in pressure (difference only due to the superposition effects described above). When permeability is pressure dependent, the same stepping generates declining pressure drop at each step due to permeability increase with pressure. Sensitivity to the initial pressure in the runs with *k(p)* helped to illustrate the non-linearity effects: the increase of initial pressure from 5000 to 6000 psi leads to similar level of the maximum injection pressure in the test simulation (9770 and 9930 psi respectively) (Figure 6). In other words, increased initial reservoir pressure may not inevitably necessitate proportionally higher injection pressure to achieve the same rate. This effect should be kept in mind in history matching of pressure sensitive reservoirs, in particular when matching SRTs in the next sections.

Downloaded from http://onepetro.org/SPEEURO/proceedings-pdf/17EURO/2-17EURO/D021S001R004/1290734/spe-185795-ms.pdf/1 by Sharisse Geiger on 01 March 2024

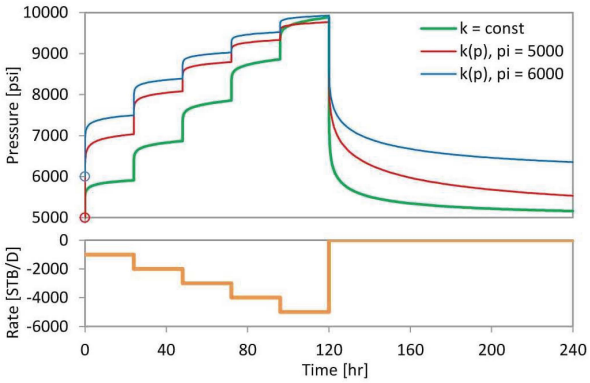


Figure 6—Synthetic SRTs numerically simulated with constant (k = const) and pressure dependent (k(p)) permeabilities. pi - initial reservoir pressure used in the runs with k(p).

An approach to Step Rate Test interpretation

Pressure and rate history from a Step Rate Test (SRT) may be interpreted at different levels. The following three components are suggested in this study and each one may be used separately or in a combination.

p-Q analysis

A *p-Q* plot may be drawn based on results of a SRT, where Q is the current step rate and p – maximum pressure at the step. The form of the *p-Q* plot will approximately indicate whether well productivity (*PI*) or injectivity (*II*) index, according to *(1)* in the appendix, is growing, declining or near to constant as discussed above. *PI* may be calculated for each step and plotted as *PI* versus pressure or rate. Different estimates for *PI* may be considered:

- A *global* estimate, where current rate is divided by difference between initial reservoir pressure and maximum pressure at current step. This estimate gives smooth change in *PI*.
- A *local* estimate, where increase in rate at current step is divided by increase in pressure at the step (the difference between maximum pressures at previous and current steps). This estimate provides focus on local changes in well-reservoir parameters for the step.
- An average of the two estimates above.

Plotting and analyzing these *PI* trends may serve as a first step in diagnostics of *PI* changes from an SRT.

Step-by-step PTA

A family of pressure transients may be extracted from the SRT and plotted in the same graph. Position and behavior of sequential pressure transients and derivatives are analyzed to diagnose changes in well-reservoir parameters. Each step' transient is analyzed using PTA, estimating well-reservoir parameters such as skin and permeability-thickness product (reservoir conductivity, *kh*). The estimated well-reservoir parameters are plotted vs pressure and/or rate, giving functions, which may be used as input for reservoir simulation.

History matching of SRT with numerical simulation

The trends / functions of well-reservoir parameters estimated from the step-by-step PTA may be tested and verified in reservoir simulation and the ability to history match SRT via introducing these trends into the simulation may be evaluated. In this study, simple single-phase flow simulations are considered to focus on matching SRT history with estimated *k(p)* from step-by-step PTA. The pressure dependent permeability *k(p)* may be introduced as exponential function described by *(4), (5)* or as a linear approximation *(6)* in the appendix. Full-scale reservoir simulation may be used to match SRT as a next step or a full alternative to the simple numerical models.

Downloaded from http://onepetro.org/SPEEURO/proceedings-pdf/17EURO/2-17EURO/D021S001R004/1290734/spe-185795-ms.pdf/1 by Sharisse Geiger on 01 March 2024

This approach was tested on the Ekofisk well data and results of the testing are discussed in the next section.

Examples of field application

The approach to SRT interpretation presented above was verified on well data from the Ekofisk field by testing in numerical simulations. Applicability, accuracy and reliability of the analytical interpretations were further analyzed based on the simulation results.

Ekofisk is a fractured carbonate field on the North Sea shelf with first production since 1971 (Hermansen, Thomas, Sylte, & Aasboe, 1997). The field was developed initially by a primary depletion drive with water flood been fully implemented in 1987. Since waterflood introduction it has always been a challenge to understand the fracture development and its impact on pattern recovery. Different natural fracture types have been detected from the comprehensive studies of Ekofisk (Agarwal, Allen, & Farrell, 1997). In these studies, the tectonic fractures (or joints, the most common type), establishing interconnected networks, were identified to govern fluid flow in the reservoir. Stress-(pressure-) dependent permeability for fractured chalk reservoirs was reported based on laboratory experiments and analysis of field data (Powley, Peng, & Ali, 1992), (Teufel, Rhett, Farrell, & Lorenz, 1993), (Shchipanov, Berenblyum, & Kollbotn, 2014). The most of new wells at Ekofisk are stimulated by generating induced fractures, which in a combination with the natural fractures govern injection and production performance at the field. Historically, the major surveillance tools to characterize reservoir in injectors' proximity were Fall-Off Test (FOT) and SRT. This makes analysis of SRTs an important component of the reservoir management.

Slanted fractured well

The first SRT example is for a slanted injection well hydraulically fractured during stimulation. The SRT (Figure 7) was conducted after a couple of days of water injection with a short shut-in following the stimulation. The SRT consisted of 14 steps with similar rate steps and duration, except the first and the final steps. The *p-Q* plot (Figure 8) from the SRT is almost linear, with minor convexity to the rate axis followed by convexity to the pressure axis, suggesting that the Injectivity Index (*II*) is fluctuating as pressure increases (Figure 9). The *local II* trend contains fluctuations up and down zooming small fluctuations of *global II* trend, which is quite smooth. It is however difficult to find stable growing or declining *II* trend.

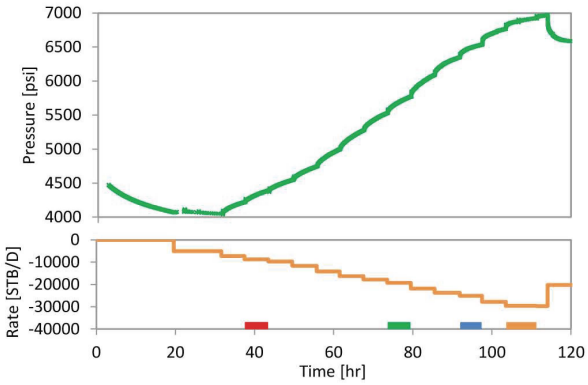


Figure 7—Step-rate test (SRT) of a slanted stimulated (induced fracture) well with steps 3, 9, 12 and 14 highlighted (to be used for reference in Figure 10).

Downloaded from http://onepetro.org/SPEEURO/proceedings-pdf/17EURO/2-17EURO/D021S001R004/1290734/spe-185795-ms.pdf/1 by Sharisse Geiger on 01 March 2024

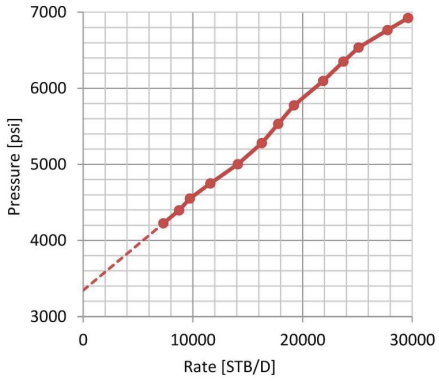


Figure 8—p-Q plot (bottom hole pressure – water injection rate) resulted from SRT in Figure 7.

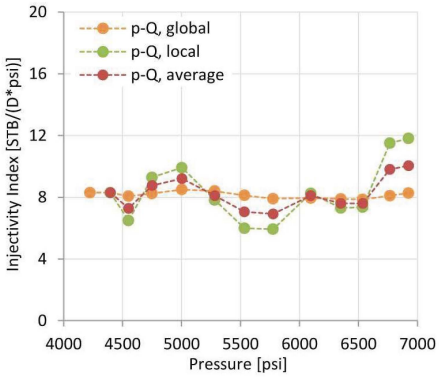


Figure 9—Three trends of Injectivity Index (II) calculated for the SRT (Figure 7 and Figure 8) using global and local estimates and average of these two estimates.

While the first 9 steps of the SRT showed quite similar pressure derivatives, this starts to change from step 10 onward (Figure 10). The pressure derivatives for steps 9, 12 and 14, shown as examples in Figure 10, each reaching stabilization at different levels, indicating that IARF regimes are establishing, but reservoir conductivity (*kh*) is different. Derivative stabilization at a lower level indicates that conductivity (*kh*) is increasing.

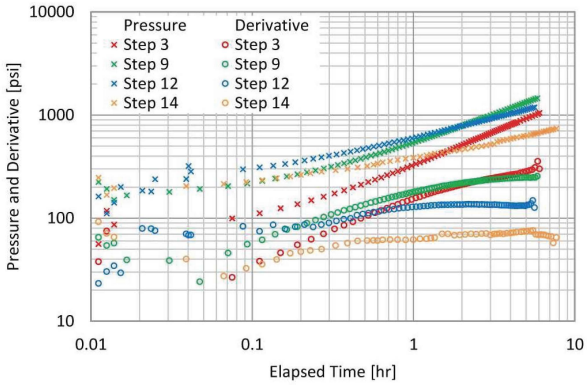


Figure 10—Pressure and derivative transients for sequential steps of the SRT in Figure 7. Similar position and behavior of the pressure derivatives in the log-log scale (steps 3 to 9) with changes at following steps: 10 to 14.

Downloaded from http://onepetro.org/SPEEURO/proceedings-pdf/17EURO/2-17EURO/D021S001R004/1290734/spe-185795-ms.pdf/1 by Sharisse Geiger on 01 March 2024

Before analyzing pressure transients at each step, analytical and numerical models with different fracture representation were compared (Figure 11 and Figure 12). In both the analytical and numerical models, two approaches to represent the induced fracture were compared: approximation of the fracture effect though negative well skin, and by explicit fracture modelling. The numerical models were made quite large to mimic the infinite reservoir assumed in the analytical models.

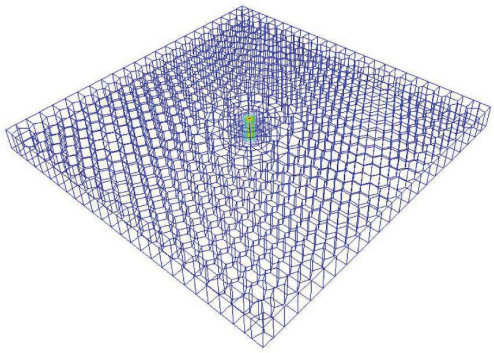


Figure 11—Numerical model of vertical injection well in reservoir segment (colors highlight pressure: red – high, blue - low).

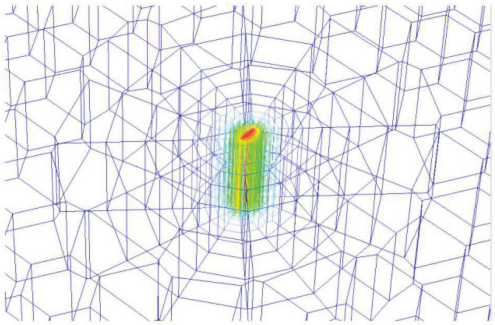


Figure 12—Numerical model of vertical fractured well in the same reservoir segment (Figure 11), zooming the near wellbore area.

Since linear flow to the induced fracture governs the well-reservoir connectivity, the well was modelled as vertical (neglecting the well inclination). Focusing on the last step of the SRT, the pressure transient (Figure 13) and SRT history (Figure 14) were simulated analytically and numerically for the two approaches of accounting for the fracture impact described above.

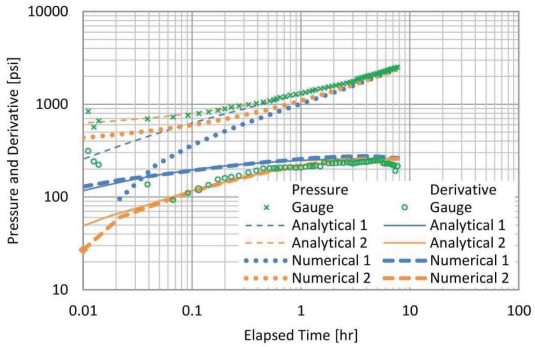


Figure 13—Actual (gauge) and simulated with analytical and numerical models (Figure 11 and Figure 12) pressure and derivative transients for step 14 in the log-log scale.

Downloaded from http://onepetro.org/SPEEURO/proceedings-pdf/17EURO/2-17EURO/D021S001R004/1290734/spe-185795-ms.pdf/1 by Sharisse Geiger on 01 March 2024

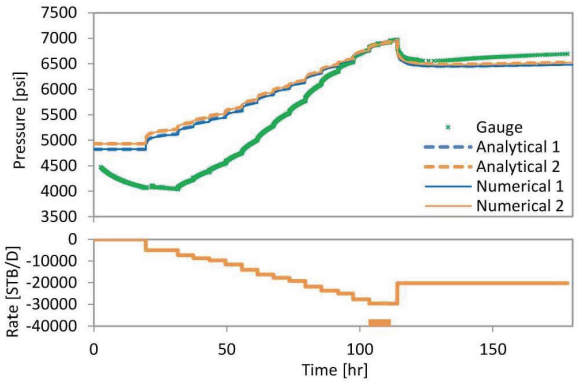


Figure 14—Analytical and numerical simulations of the SRT (Figure 7) using model with skin (1) and induced fracture and fracture skin (2), Figure 13. The reference step 14 is highlighted.

Although the explicit fracture modelling gave better matching of the actual pressure derivative than the negative skin approach (Figure 13), the deviation in simulated SRT history was quite small (Figure 14). The total skin was the same in both cases causing similar model' response on the history scale. Also, the results of both the analytical and the numerical models almost coincide for the same representation of the fracture. Based on this comparison, the less complicated case to represent the fracture via negative well skin was selected for the following step-by-step interpretations and SRT simulations.

Application of the step-by-step PTA to the SRT consisted of analytical interpretation of pressure and derivative transients at each step to estimate well-reservoir parameters of the selected model: constant well skin and reservoir conductivity (*kh*). Since the derivatives from step 9 through step 14 are quite different from previous steps (Figure 10), results of the interpretation are also different. Analyses of steps 3 and 14 illustrate the step-by-step PTA with analytical models. Taking step 3 as the first reference, tuning the model parameters (*kh* and *S*) provided reasonable match of the observed pressure transient and its derivative, while the same model with parameters tuned to match step 14 gave mismatch of step 3 (Figure 15). The same effect was observed when matching step 14 (Figure 16). In this SRT example, the analytical model with constant parameters (*kh* and *S*) is capable of matching only the step in focus, but not other steps (for steps 9-14).

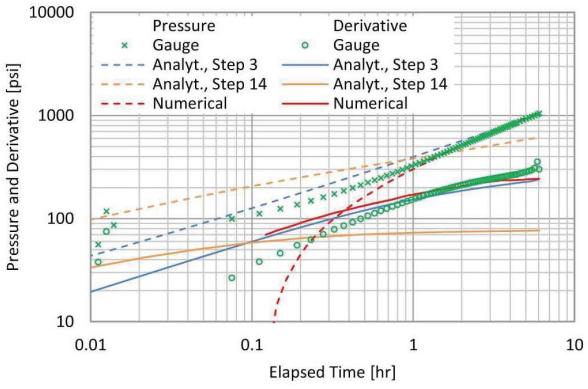


Figure 15—Trying to match response of step 3 with analytical models tuned to steps 3 and 14 and numerical model with function k(p) obtained from the step-by-step interpretation of all steps and tuned skin (Figure 17).

Downloaded from http://onepetro.org/SPEEURO/proceedings-pdf/17EURO/2-17EURO/D021S001R004/1290734/spe-185795-ms.pdf/1 by Sharisse Geiger on 01 March 2024

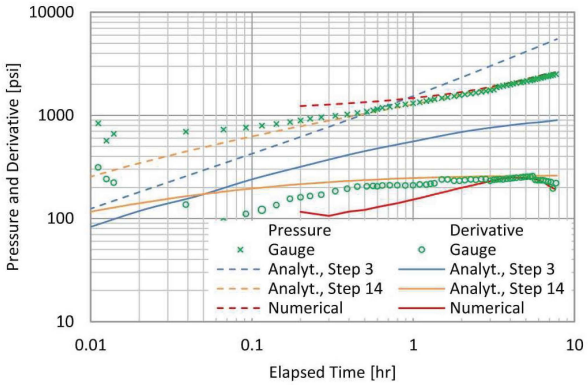


Figure 16—Trying to match response of step 14 with analytical models tuned to steps 3 and 14 and numerical model with the function k(p) described above (Figure 15).

As a result of the step-by-step interpretation with the analytical model, trends of well skin and reservoir conductivity were estimated (Figure 17). Assuming constant pay thickness (h), kh as a function of p may be transformed into a $k(p)$ function. The PTA interpretation also gave an estimate of II at each step ('PTA' in Figure 18), while the estimated skin and conductivity may serve as a basis for alternative II calculation using the relationships *(3), (7)* and *(8)* in the appendix ('$kh+S$' in Figure 18). It seems that II estimated from the PTA interpretation is more accurate than the '$kh+S$' estimate due to the assumption of constant pressure at the external radius used in the relationships *(3), (7)* and *(8)*. These two estimates are compared to the average II trend estimated from the p-Q plot (Figure 9), which is close to the PTA trend confirming possibility to use p-Q diagram as a diagnostic tool for detecting changes in well injectivity (productivity).

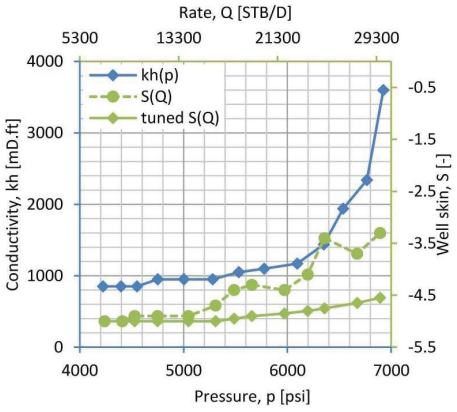


Figure 17—Reservoir conductivity (kh) as function of pressure (p) and well skin factor (S) as function of rate (Q) – output of the step-by-step interpretation of all steps of the SRT (Figure 15, Figure 16) and the skin adjusted to match SRT with k(p). Assuming constant pay thickness (h), k(p) may be found.

Downloaded from http://onepetro.org/SPEEURO/proceedings-pdf/17EURO/2-17EURO/D021S001R004/1290734/spe-185795-ms.pdf/1 by Sharisse Geiger on 01 March 2024

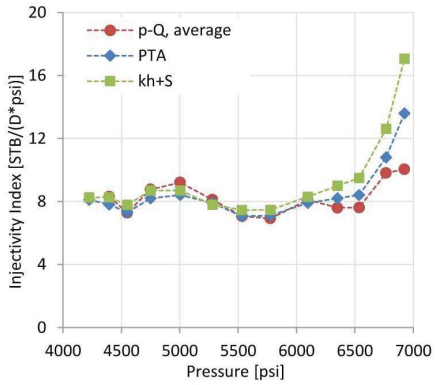


Figure 18—Injectivity index variation with increasing pressure (step to step) obtained from the p-Q plot analysis (Figure 8, Figure 9) compared to two variations obtained by the step-by-step PTA and calculated from steady-state flow approximation based on reservoir conductivity and skin estimates (kh+S).

The results from the step-by-step PTA: pressure dependent permeability, *k(p)*, and skin, *S*, were tested in numerical simulation (Figure 11). Introducing the estimated *k(p)* function (Figure 17), while keeping skin constant (estimated from the first step), gave an overestimation of flow capacity in the numerical simulations (Figure 19). In turn, combining *k(p)* with *S(Q),* both estimated from the step-by-step PTA, provided underestimation of the capacity and fluctuating pressure response at higher rates (Figure 19). Further tuning of *S(Q)* as shown in Figure 17 resulted in a reasonable match of the whole SRT sequence (Figure 19).

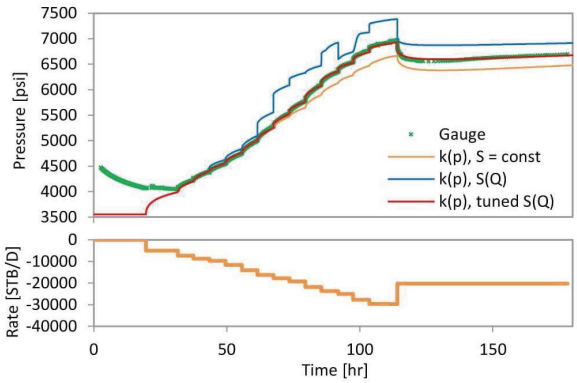


Figure 19—Trying to match the SRT (Figure 7) with numerical models accounting for pressure dependent permeability, k(p), and different skins (Figure 17): constant (S = const); resulted from the step-by-step interpretation (S(Q)); and adjusted to get better SRT match, (tuned S(Q)).

The finally matched model with *k(p)* and *S(Q)* (Figure 19) was compared to the model with constant *k* and *S* estimated for 3rd and 14th steps (Figure 20). Comparison of these cases in log-log scale may be found in Figure 15, Figure 16, where the analytical model was employed for the cases with constant parameters. Both linear and log-log scale comparisons revealed inability to match all steps with constant parameters, while combining *k(p)* and *Q(S)* provided such a capability. The numerical model with *k(p)* estimated from the step-by-step PTA is capable of matching all steps, including pressure derivative (Figure 15, Figure 16, Figure 19).

Downloaded from http://onepetro.org/SPEEURO/proceedings-pdf/17EURO/2-17EURO/D021S001R004/1290734/spe-185795-ms.pdf/1 by Sharisse Geiger on 01 March 2024

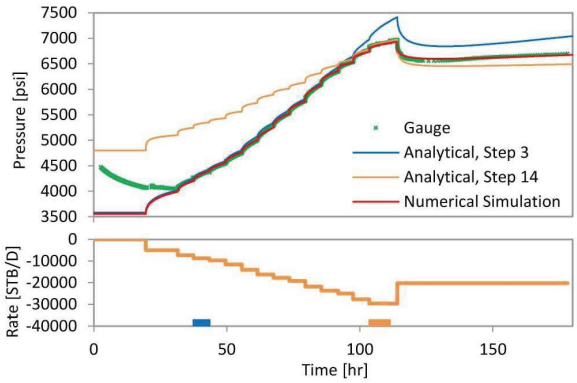


Figure 20—Trying to match the SRT (Figure 7) with analytical models with constant reservoir conductivity (kh) and skin (S) tuned to 3rd and 14th steps (Figure 15, Figure 16) and with numerical model with k(p) from the step-by-step interpretation and tuned skin (Figure 18).

Summarizing the results of the slanted well example, the following may be concluded:

- The *p-Q* analysis is fast and simple and may be used to reveal changes in well injectivity (productivity), *e.g.* using three *PI* approximations described above. The injectivity combines both well (skin) and reservoir (conductivity) effects, which may mask changes of each other. In this example, the conductivity increase was masked by the skin increase preventing from monotonic growth of injectivity, *i.e.* such changes in parameters are compensated when estimating injectivity.
- The capability to estimate *k(p)* from the step-by-step PTA that may be directly applied in reservoir simulation has been confirmed. This PTA technique enables separating well (skin) from reservoir (conductivity) effects, which is crucial for performance forecast. This is an advantage comparing to *p-Q* analysis, especially in the case of the masking effect described above.
- Applying the step-by-step PTA to estimate well skin changes is not straight forward. In this example, estimated skin increased significantly from step to step (indicating less well stimulation effect) with some fluctuations. The skin tuned to provide the SRT match was moderately increasing without fluctuations (Figure 17). Appearance of an artificial positive skin in interpretations of SRTs numerically simulated with zero skin was also reported in (Alaassar, 2015).

The artificial skin effect requires special attention and we suggest the following explanation. The effect is apparently related to the superposition principle (described above) used in PTA to simulate and interpret pressure responses. In the case of step-by-step interpretation, when superposing a current step pressure response with previous steps, the contribution of the previous steps is calculated based on *kh* and *S* estimated for the current step. If *kh* and/or *S* are changing from step to step, this leads to under or overestimation of this contribution. In the case of increasing permeability, previous steps actually contribute with higher pressure drop (permeability at previous steps is lower than at the current step) than it would be for constant permeability level at the current step. This may be misinterpreted as an additional skin, which is obviously not present. The effect would grow as the number of steps increases. Therefore, number of steps in a SRT may be managed by the balance between knowledge and details we are getting (more steps is better) and controlling the artificial skin effect (less steps is better). On the other hand, an interpretation technique to remove this artificial skin may be also elaborated.

Horizontal multi-fracture well

The second example is a horizontal injection well with multiple induced fractures generated during multi-stage stimulation. The stimulation effect for a horizontal well may also be described by a negative skin. In

Downloaded from http://onepetro.org/SPEEURO/proceedings-pdf/17EURO/2-17EURO/D021S001R004/1290734/spe-185795-ms.pdf/1 by Sharisse Geiger on 01 March 2024

general, pressure derivative for such a well should have early and late IARF regimes in a combination with two linear flow regimes, Figure 21 ((Bourdet, 2002), (Houze, Viturat, & Fjaere, 2011)).

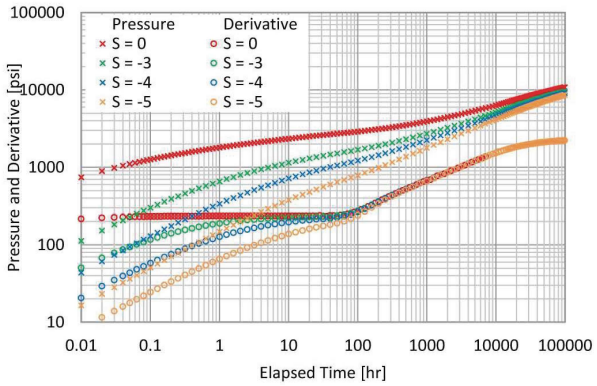


Figure 21—Injection pressure and derivative transients for horizontal well with different skin effects (S) reflecting the well stimulation (S < 0).

In reality, it is though often difficult to observe the late IARF regime due to interference from nearby wells, caused by distance between the wells being shorter than the well lengths. The early IARF regime may however be observed in pressure derivatives for negative skin until a certain value (Figure 21), while for lower skins (better stimulation) this IARF regime could be masked by transition from the first ½ slope derivative period (stimulation or linear flow to induced fractures) to the second ½ slope period (linear flow to horizontal wellbore). In this case, estimation of reservoir conductivity and skin becomes ambiguous.

This ambiguity may be illustrated by the examples in Figure 22, where permeability is twice higher in the second example, while skin is higher in the first example. During the first day the responses are quite similar, providing the same final pressure drop at 24 *hr*. This argues for the importance of observing the early IARF or at least the well-recognized cavity in the derivative that may be interpreted as completion of the IARF regime.

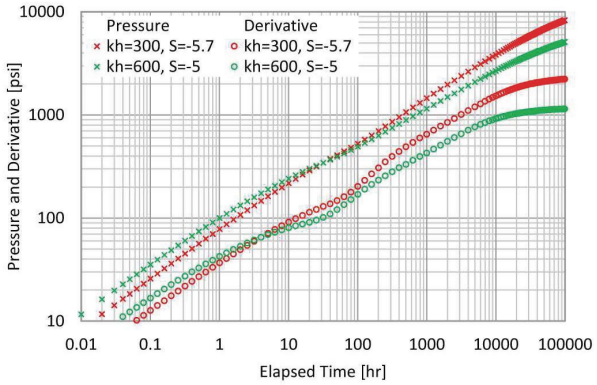


Figure 22—Injection pressure and derivative transients for horizontal well with different skins (S = -5 and -5.7) in reservoir with different conductivity (300 and 600 mD.ft).

The SRT in focus (Figure 23) was carried out after two-months of well shut-in (pressure fall-off) following one year of water injection. The *p-Q* plot from the SRT (Figure 24) has a change in slope after the second step confirmed by a jump in the injectivity trend at 3rd step (Figure 25). Comparison of the pressure and derivative transients at sequential steps (Figure 26) argues for significant increase of the complex

Downloaded from http://onepetro.org/SPEEURO/proceedings-pdf/17EURO/2-17EURO/D021S001R004/1290734/spe-185795-ms.pdf/1 by Sharisse Geiger on 01 March 2024

parameter kh_w at step 3, where k is reservoir permeability (assumed to be equal in vertical and horizontal directions) and h_w is effective well length. This is in agreement with the diagnostics form the p-Q analysis (Figure 24, Figure 25). Analogically to the slanted well example above, the step-by-step PTA (Figure 27 and Figure 28) resulted in pressure dependent conductivity (Figure 29) with skin variation in the range of -5.4 to -5.0. The effective well length, h_w, and reservoir pay thickness, h, were assumed to be constant in this analysis providing estimation of $k(p)$ function.

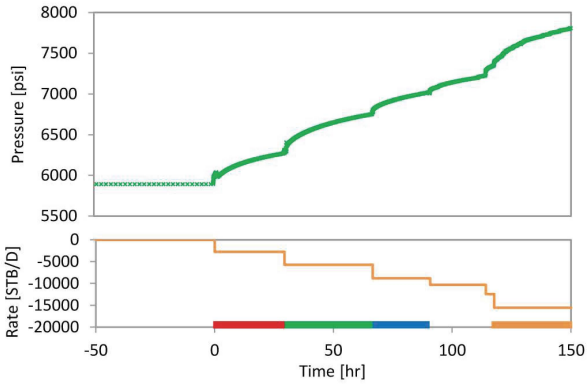


Figure 23—Step-rate test (SRT) of a horizontal stimulated (multiple induced fractures) well with steps 1, 2, 3 and 5 highlighted.

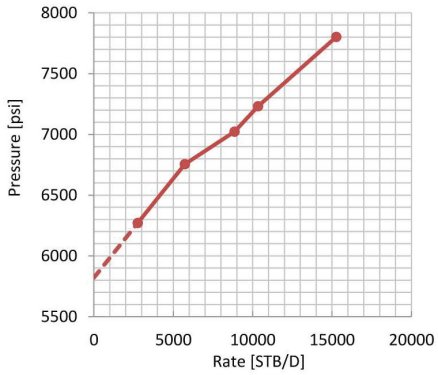


Figure 24—p-Q plot resulted from the SRT in Figure 23.

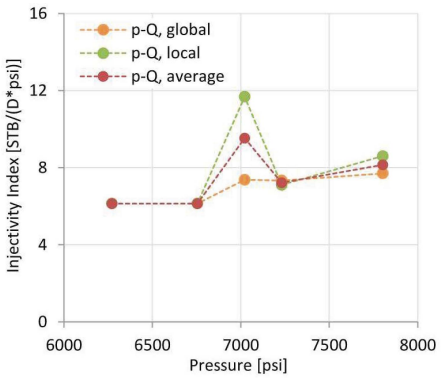


Figure 25—Three trends of Injectivity Index (II) calculated using global and local estimates for the SRT (Figure 23, Figure 24) and average of these two indices.

Downloaded from http://onepetro.org/SPEEURO/proceedings-pdf/17EURO/2-17EURO/D021S001R004/1290734/spe-185795-ms.pdf/1 by Sharisse Geiger on 01 March 2024

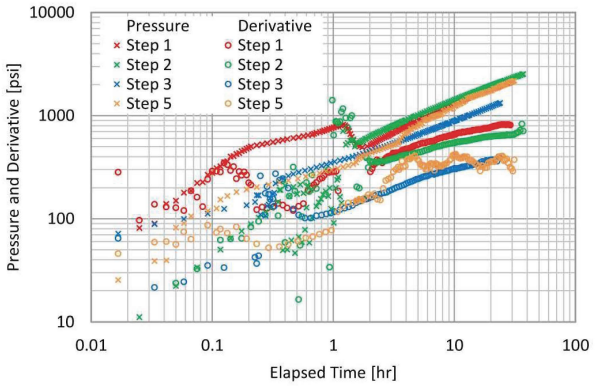


Figure 26—Pressure and derivative transients for sequential steps of the SRT in Figure 23. Similar position and behavior of the pressure derivatives in log-log scale (steps 1 and 2) with significant change at steps 3, 5.

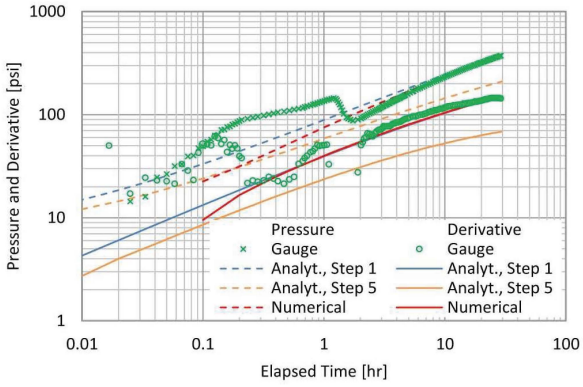


Figure 27—Trying to match response of step 1 with analytical models tuned to steps 1 and 5 and numerical model with kh(p) obtained from the step-by-step interpretation of all steps (Figure 29) and constant (average) skin estimate.

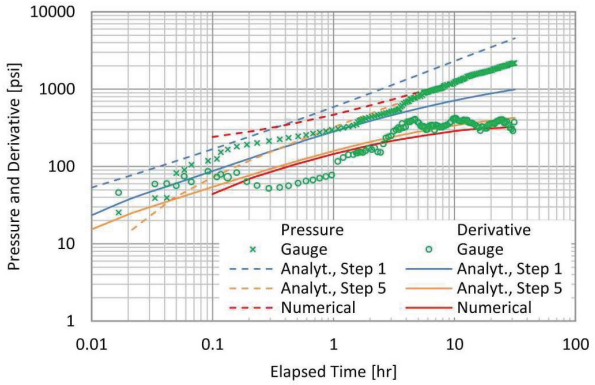


Figure 28—Trying to match response of step 5 with analytical models tuned to steps 1 and 5 and the numerical model described in Figure 27.

Downloaded from http://onepetro.org/SPEEURO/proceedings-pdf/17EURO/2-17EURO/D021S001R004/1290734/spe-185795-ms.pdf/1 by Sharisse Geiger on 01 March 2024

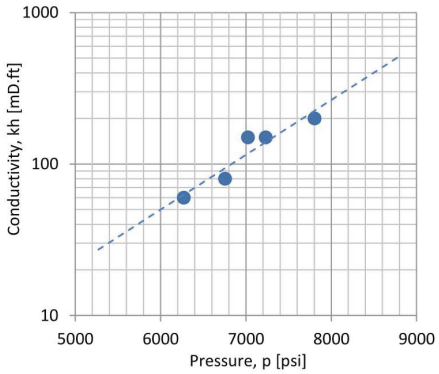


Figure 29—Reservoir conductivity (kh) as function of pressure (p) resulted from the step-by-step interpretation of all steps of the SRT (Figure 28).

This pressure dependent conductivity function (Figure 29), together with average skin for the range above were introduced in numerical simulation (Figure 30), providing reasonable match of the SRT history (Figure 31) and pressure and derivatives at each step (Figure 27, Figure 28). An equivalent numerical simulation with explicit fracture modeling was also tested (Figure 32). Similar (to the fracture effect via skin model) history match of the SRT was achieved with 7 fractures specified with half-length of 80 *ft*. The numerical model (Figure 30) may be employed to forecast pressure drop for higher rates (Figure 33) and to extrapolate the *p-Q* plot (Figure 34).

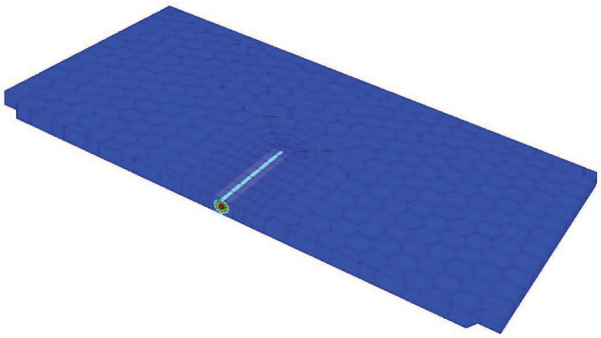


Figure 30—Numerical simulation of the horizontal well, where negative skin reflects the well stimulation impact.

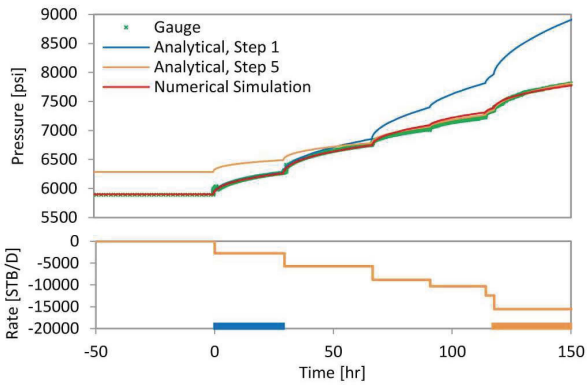


Figure 31—Analytical and numerical simulations of the SRT (Figure 23) using analytical model tuned to steps 1 and 5 and numerical model (Figure 30) capable of matching all the steps. Reference steps 1 and 5 are highlighted.

Downloaded from http://onepetro.org/SPEEURO/proceedings-pdf/17EURO/2-17EURO/D021S001R004/1290734/spe-185795-ms.pdf/1 by Sharisse Geiger on 01 March 2024

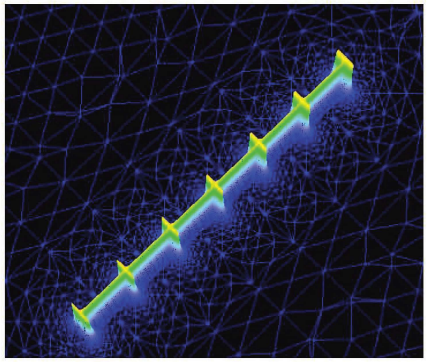


Figure 32—Numerical simulation of the horizontal well with multiple induced fractures. 3D block-edge visualization of 2D pressure simulation results in red-blue scale: red - high pressure, blue - low pressure.

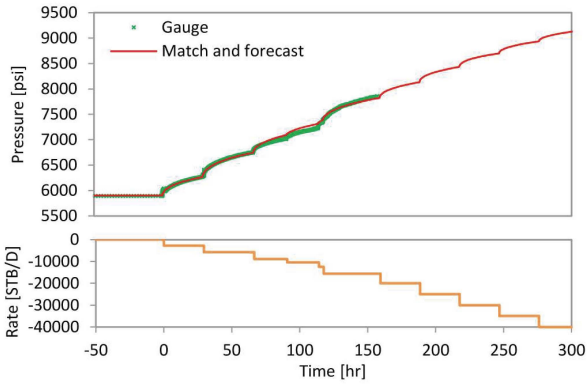


Figure 33—Matching the SRT (Figure 31) and forecasting pressure growth at higher rates using the numerical model (Figure 30) and the kh(p) function (Figure 29).

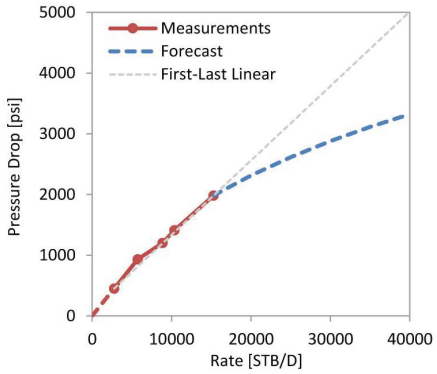


Figure 34—p-Q plot from the numerical simulation results (Figure 33).

The question of ambiguity in interpretation of horizontal well response requires special attention. Alternative interpretations are possible. Also, as discussed above, the modelling of a well stimulation using the skin concept is an approximate method and the derivative behavior at early time may be reproduced with different models.

As an alternative interpretation, the conductivity, *kh*, estimated from the constant derivative level (IARF) may be prioritized as illustrated in Figure 35. In this case, the conductivity is estimated from IARF regime applying zero skin ('IARF' case in Figure 35). Further tuning of skin provides correct pressure drop, even if

Downloaded from http://onepetro.org/SPEEURO/proceedings-pdf/17EURO/2-17EURO/D021S001R004/1290734/spe-185795-ms.pdf/1 by Sharisse Geiger on 01 March 2024

such a tuning led to deviation from the observed derivative ('IARF+Skin' in Figure 35). This interpretation gave an alternative *kh(p)* function (Figure 37). Rate or time dependent skin may be also employed in attempting to match the SRT response, although physical meaning and application in reservoir simulation of such an approach requires additional considerations, which are not covered in this paper. Thus, keeping the conductivity constant (the same as interpreted from the first step of the base case interpretation, Figure 29) and tuning skin, pressure response at each step may be matched ('Variable skin' in Figure 36). Comparison of these alternative interpretations on the example of matching step 3 (Figure 36) showed that the base case interpretation ('Best Match') provided reasonable match of both pressure transient and its derivative, while the alternative interpretations - only match of pressure drops, but not the observed derivatives. It should be noted, that in the case of rate or time dependent skin the support point in the derivative analysis, that is the IARF regime and constant derivative in the case of conductivity estimations, is lost.

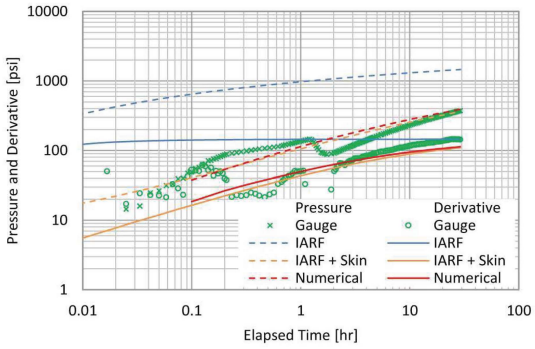


Figure 35—Trying to match step 1: alternative interpretation acknowledging IARF as final constant derivate period: IARF with zero skin (IARF), tuning skin to match pressure drop (IARF + Skin) and numerical model based on the tuned skin results.

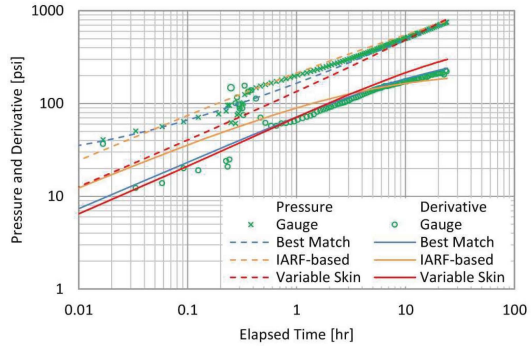


Figure 36—History matching of step 3 with alternative interpretations.

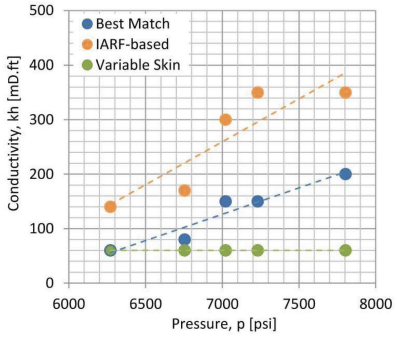


Figure 37—Comparison of reservoir conductivity trends obtained with three alternative interpretations.

Downloaded from http://onepetro.org/SPEEURO/proceedings-pdf/17EURO/2-17EURO/D021S001R004/1290734/spe-185795-ms.pdf/1 by Sharisse Geiger on 01 March 2024

Reservoir conductivity and skin estimated for each step of the SRT using the alternative interpretations are summarized by plotting versus pressure in Figure 37 and Figure 38. Both cases with increasing conductivity provided similar trends with shifting upward in the 'IARF-based' case (Figure 37). Skin estimations for these two cases follow similar downwards trends in Figure 38, where additional positive skin from step to step seems to be related with the artificial skin discussed above (the skin axis here has inverse order to the axis in Figure 17). Both *k(p)* functions in combination with corresponding skin provide reasonable match of the SRT with numerical simulation (Figure 39), but with some deviation from the observed derivative in log-log scale for the alternative interpretation (Figure 35, Figure 36). If conductivity is fixed, declining negative skin is required to match the SRT (Figure 38). These alternative results may be considered as uncertainty of the SRT interpretation and integrated into reservoir simulation, such as forecasting of injection scenarios may also include uncertainty evaluation. This evaluation may be a useful component in analysis of stimulated horizontal wells, where the unique interpretation is difficult.

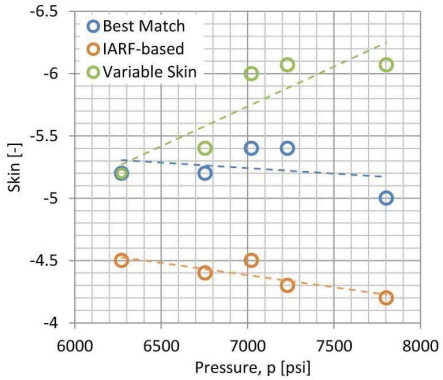


Figure 38—Comparison of well skin trends obtained with three alternative interpretations.

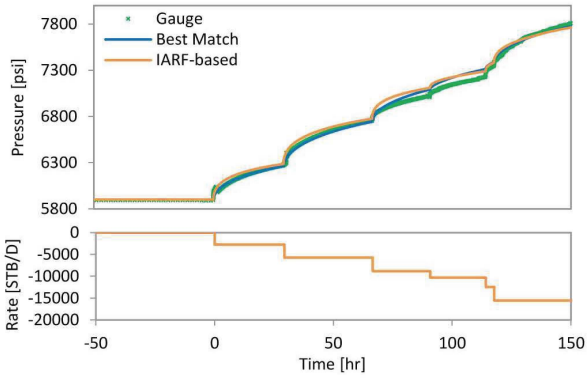


Figure 39—Numerical simulations of the SRT (Figure 23) using the numerical model with two alternative k(p) functions (Figure 37) and skin estimates (Figure 38).

Summarizing the results of the horizontal well example, the following may be concluded:

- Detecting *II* changes is possible from the *p-Q* analysis, where following step-by-step PTA confirmed detected *II* increase.
- Well-reservoir parameters resulted from the step-by-step PTA provided fast match of both pressure and derivative in the numerical models.

Downloaded from http://onepetro.org/SPEEURO/proceedings-pdf/17EURO/2-17EURO/D021S001R004/1290734/spe-185795-ms.pdf/1 by Sharisse Geiger on 01 March 2024

- Both numerical models with representing the well stimulation via skin and explicit modelling of multiple induced fractures were easily matched based on the analytical PTA results. The second model may give a reference for appropriate fracture parameters at given fracture number.
- The numerical models matched to the SRT history are capable of forecasting well performance at higher rates / pressures, where uncertainty evaluation may also be included as discussed above.

Discussion

Reservoir conductivity (kh), which includes permeability and pay thickness, is the main parameter resulted from the interpretations of IARF regimes discussed above. The pay thickness was assumed to be constant, that helped in separating and applying in reservoir simulation the pressure dependent permeability. In reality, the pay thickness may change at increasing rate, *e.g.* due to opening of high conductive features (as super-k layers, natural fractures or fracture corridors) and contribution of different layers may vary depending on rate in the case of commingled injection or production. Injection (production) logging at different well rates may help in addressing this problem. History matching of SRT data accounting for varying pay thickness and contribution of different layers may be a further step in the studies.

When considering horizontal wells, the first IARF regime may be used to estimate permeability - effective well length product (kh_w), while the second IARF - reservoir conductivity kh. Since the second IARF is difficult to observe in practice, permeability estimation mainly relies on the first IARF regime and effective well length governs permeability values obtained. The interpretations above resulted in growing kh_w at increasing rate/pressure and this growth was related with permeability increase assuming invariability of the length. At the same time, the effective well length may also vary with growing rate, time *etc., e.g.* heterogeneities in reservoir pressure distribution near wellbore may be a reason for such variation. Again, combining PTA with additional interpretations (*e.g.* 4D seismic) may help in reducing this uncertainty.

Conclusions

The following results and conclusions may be drawn from the study:

- The p-Q plot may serve as an efficient diagnostic tool for detecting changes in well injectivity or productivity.
- Step-by-step PTA, providing separation of well and reservoir effects, is a reliable interpretation technique to estimate pressure dependent reservoir conductivity (permeability).
- Results of the step-by-step PTA can be directly applied in reservoir simulation providing history matching of SRTs, which is not achievable in simulations with constant reservoir permeability.
- For pressure-(stress-) sensitive reservoirs, estimation of well skin variable with rate (pressure) is complicated by the artificial skin effect, growing with number of steps and changes in permeability.

As practical guidelines for designing and conducting SRTs in pressure-sensitive formations the following may be suggested:

- Using limited number of steps to reduce the artificial skin effect in SRT interpretations (a reasonable number of steps may be suggested as 3-7).
- In designing SRT, establishing of the IARF regime at each step should be prioritized. Here simple analytical models and preliminary knowledge of well and reservoir in focus may be used.
- Keeping the same duration and rate stepping at each step makes following analysis simpler and improves reliability of interpretation results. Here, equal rate stepping is less crucial than equal step durations.

Downloaded from http://onepetro.org/SPEEURO/proceedings-pdf/17EURO/2-17EURO/D021S001R004/1290734/spe-185795-ms.pdf/1 by Sharisse Geiger on 01 March 2024

Acknowledgments

The authors gratefully acknowledge T.A. Rolfsvåg, S. Ozoglu-Topdemir, O. Eeg and J.R. Versteeg for their contribution to the study and critical view on the interpretation results reflected in the discussion above.

The authors acknowledge ConocoPhillips Skandinavia AS and the PL018 coventurers including TOTAL E&P Norge AS, ENI Norge AS, Statoil Petroleum AS and Petoro AS for the permission to publish this paper. The research centre COREC is acknowledged for supporting development of the methodology presented. The interpretations and conclusions presented in this paper are those of the authors and not necessarily those of ConocoPhillips, nor the PL018 partners including TOTAL, ENI, Statoil and Petoro.

References

Agarwal, B., Allen, L., & Farrell, H. (1997). Ekofisk Field Reservoir Characterization: Mapping Permeability Through Facies and Fracture Intensity (SPE 35527). *SPE Formation Evaluation*, **12**(4). doi: 10.2118/35527-PA

Alaassar, M. (2015). *Simulation and Interpretation of Well Tests in Pressure (Stress) Sensitive Reservoirs with Induced Fractures*. Stavanger, Norway: Master's thesis, University of Stavanger.

Bourdet, D. (2002). *Well Test Analysis: The Use of Advanced Interpretation Models*. Elsevier.

Craig, D., & Blasingame, T. (2006). Application of a New Fracture-Injection/Falloff Model Accounting for Propagating, Dilated, and Closing Hydraulic Fractures (SPE 100578). SPE Gas Technology Symposium. Calgary, Canada, 15-17 May 2006. doi: 10.2118/100578-MS

Economides, M., Buchsteiner, H., & Warpinski, N. (1994). Step-Pressure Test for Stress-Sensitive Permeability Determination (SPE 27380). SPE Formation Damage Control Symposium. Lafayette, Louisiana, 7-10 February. doi: 10.2118/27380-MS

Egya, D., Geiger, S., Corbett, P., Bisdom, K., Bertotti, G., & Bezerra, H. (2016). Assessing the Validity and Limitations of Dual-porosity Models Using Geological Well Testing for Fractured Formations. 78th EAGE Conference & Exhibition. Vienna, Austria, 30 May - 2 June.

Elshahawi, H., & Gad, K. (2001). Estimation of Skin for High Deliverability Gas Well Tests (SPE 68144). SPE Middel East Oil Show. Bahrain, 17-20 March. doi: 10.2118/68144-MS

Hegre, T., & Larsen, L. (1994). Productivity of Multifractured Horizontal Wells (SPE 28845). European Petroleum Conference. London, U.K., 25-27 October 1994. doi: 10.2118/28845-MS

Hermansen, H., Thomas, L., Sylte, J., & Aasboe, B. (1997). Twenty Five Years of Ekofisk Reservoir Management (SPE 38927). SPE Annual Technical Conference and Exhibition. San Antonio, Texas, 5-8 October. doi: 10.2118/38927-MS

Houze, O., Viturat, D., & Fjaere, O. (2011). *Dynamic Data Analysis*. KAPPA.

Lacy, L., & Hudson, H. (1995). New Step-Rate Test Analysis for Fracture Evaluation (SPE 29591). Low Permeability Reservoirs Symposium. Denver, Colorado, 19-22 March. doi: 10.2118/29591-MS

Lizak, K., Bartko, K., Self, J., Izquierd, G., & Al-Mumen, M. (2006). New Analysis of Step-Rate Injection Tests for Improved Fracture Stimulation Design (SPE 98098). SPE International Symposium and Exhibition on Formation Damage Control. Lafayette, Louisiana, 15-17 February. doi: 10.2118/98098-MS

Powley, K., Peng, C., & Ali, N. (1992). Simulation of a North Sea Chalk Reservoir With Dynamic Rock and Natural Fracture Properties: Case Study of the Valhall Field (SPE 24914). SPE Annual Technical Conference and Exhibition. Washington, DC, 4-7 October. doi: 10.2118/24914-MS

Salazar, A., & Kumar, A. (1992). Case Histories of Step Rate Tests in Injection Wells (SPE 23958). Permian Basin Oil and Gas Recovery Conference. Midland, Texas, 18-20 March. doi: 10.2118/23958-MS

Shchipanov, A., Berenblyum, R., & Kollbotn, L. (2014). Pressure Transient Analysis as an Element of Permanent Reservoir Monitoring (SPE-170740). SPE Annual Technical Conference and Exhibition. Amsterdam, The Netherlands, 27-29 October. doi: 10.2118/170740-MS

Singh, P., & Agarwal, R. (1990). Two-Step Rate Test: New Procedure for Determining Formation Parting Pressure (SPE 18141). *Journal of Petroleum Technology*, **42**(1). doi: 10.2118/18141-PA

Singh, P., Agarwal, R., & Krase, L. (1987). Systematic Design and Analysis of Step-Rate Tests To Determine Formation Parting Pressure (SPE 16798). SPE Annual Technical Conference and Exhibition. Dallas, Texas, 27-30 September. doi: 10.2118/16798-MS

Teufel, L., Rhett, D., Farrell, H., & Lorenz, J. (1993). Control of Fractured Reservoir Permeability by Spatial and Temporal Variations in Stress Magnitude and Orientation (SPE 26437). SPE Annual Technical Conference and Exhibition. Houston, Texas, 3-6 October. doi: 10.2118/26437-MS

Downloaded from http://onepetro.org/SPEEURO/proceedings-pdf/17EURO/2-17EURO/D021S001R004/1290734/spe-185795-ms.pdf/1 by Sharisse Geiger on 01 March 2024

Appendix

$$PI = \frac{\Delta p}{Q}, \tag{1}$$

$$\Delta p = p_e - p_w, \tag{2}$$

$$\Delta p = p_i - p_w, \tag{3}$$

$$\gamma = \frac{1}{k}\frac{\Delta k}{\Delta p}, \tag{4}$$

$$k = k^{ref} \exp\left[\gamma\left(p - p^{ref}\right)\right], \tag{5}$$

$$k = k^{ref}\left[1 + \gamma\left(p - p^{ref}\right)\right], \tag{6}$$

$$Q = \frac{2\pi kh}{\mu B\left[\ln {r_e}/{r_w} + S\right]}\Delta p, \tag{7}$$

$$PI = \frac{2\pi kh}{\mu B\left[\ln {r_e}/{r_w} + S\right]}, \tag{8}$$

where PI is productivity (injectivity) index, Δp - pressure drop, Q - injection rate at reservoir conditions, p_w - well flowing pressure, p_e and p_i - pressure at external boundary and initial reservoir pressure, γ - permeability modulus, k - permeability, k^{ref} - permeability at reference pressure p^{ref}, h - reservoir pay thickness, μ - fluid viscosity, r_w and r_e - well and external radii, S - well skin, B - formation volume factor.

Downloaded from http://onepetro.org/SPEEURO/proceedings-pdf/17EURO/2-17EURO/D021S001R004/1290734/spe-185795-ms.pdf/1 by Sharisse Geiger on 01 March 2024